

# ENGINEERING JOURNAL

*Article*

## Sensitivity Analysis of Coastal Flooding to Geographical Factors: Numerical Model Study on Idealized Beaches

Chanyut Kalakan<sup>1</sup>, Anurak Sriariyawat<sup>2</sup>, Sittichai Naksuksakul<sup>3</sup>,  
and Thamnoon Rasmeemasuang<sup>1,\*</sup>

<sup>1</sup> Department of Civil Engineering, Faculty of Engineering, Burapha University, Chon Buri 20131 Thailand.

<sup>2</sup> Department of Water Resources Engineering, Faculty of Engineering, Chulalongkorn University, Bangkok 10330 Thailand.

<sup>3</sup> Geo-Science & Petroleum Engineering Research Department, PTT Research and Technology Institute, Ayutthaya 13170 Thailand.

\*E-mail: [thamnoon@eng.buu.ac.th](mailto:thamnoon@eng.buu.ac.th) (Corresponding author)

**Abstract.** This study evaluated the potential of coastal trees to reduce flooding areas caused by waves with abnormal heights, such as storm surges, using a numerical model applied to idealized beaches. The study considered 5 factors that affect sensitivity of coastal areas to flooding: slope of the beach, bottom friction coefficient, length of tree lines, width of tree lines, and shape of tree areas. The results indicate that slope of the beaches can reduce flooding areas, as steep slopes can transform wave energy into potential energy. With regard to the friction coefficient, beaches with higher bottom friction factors will have fewer flooding areas. Relative to beaches with no trees at all, increasing the length and width of tree lines can reduce flooding areas by as much as 30%. However, the shapes of tree areas have no significant effect on flooding areas.

**Keywords:** Coastal flooding, coastal vegetation, friction factor.

ENGINEERING JOURNAL Volume 20 Issue 1

Received 2 December 2014

Accepted 4 August 2015

Published 29 January 2016

Online at <http://www.engj.org/>

DOI:10.4186/ej.2016.20.1.1

## 1. Introduction

Coastal flooding is a natural disaster that occurs in coastal areas when the mass of seawater overwhelms or floods the land along the coastal line, particularly low-lying land. Coastal flooding usually occurs when storm surges or tsunamis approach the coast. The severity of flooding may be intensified during high tides or spring tides. In addition, the severity of coastal flooding is slowly being affected by climate change, which likely causes sea level rise [1, 2], and land subsidence due to overuse of groundwater.

Coastal inundation caused by storm surges is a topic of great interest to researchers because it is such a severe and frequent natural disaster that it is classified as a coastal disaster with high risk. Storm surges are waves that occur when tropical cyclones approach coasts. Low pressure at the center of a tropical cyclone raises the sea level higher than normal, creating large water domes that approach the coasts. Moreover, tropical cyclones approach the coast with very high wind velocities, intensifying the severity of surges. Tropical cyclones and storm surges can be severe enough to demolish houses, uproot trees, and destroy the properties of people living in coastal areas, in addition to causing coastal flooding. In addition, studies indicate that global climate change is increasing the severity of storm surges [3].

Studies of storm surges and coastal flooding have mostly been conducted using numerical models, because field studies or experiments during storms are much more difficult to perform. Therefore, researchers collect field data or traces of evidence after storm incidents for further analysis using mathematical models. There are fewer studies of flooding due to storm surges than there are of storm surges alone. Such studies emphasize developing mathematical models to simulate the actual storm surges caused by tropical cyclones. These studies focus on different aspects of the model, such as developing modules or algorithms that offer more accurate calculations [4–11], explaining the effects of hydrodynamic factors on storm surges [8, 11–13], or developing databases of storm surges for use forecasting future incidents [14, 15], particularly under the pressures of global climate change and sea level rise [16].

Measures to reduce damage from storm surges may be achieved by using coastal structures such as dikes or floodgates as shelters from storm surges [17]. However, such measures may not be economically suitable for certain countries with long coastal lines or for countries that are rarely affected by such natural disasters. The most effective measure to implement first is to warn people living near coasts to evacuate risky areas efficiently and in a timely manner. Another sustainable measure is to build or restore natural shelters, such as tree lines or coastal vegetations as well as coastal wetlands.

Several studies on the potential of coastal tree lines and coastal wetlands to reduce wave energy and flooding areas due to large waves have been published, particularly due to and following the Indian Ocean tsunami of 2004 [18–21]. In cases relating to storm surges and the subsequent flooding, most studies apply storm surge models along with hydrodynamic models to simulate coastal flooding, and then compare the simulated results with data obtained by field surveys [22–24]. Most study results consistently show that coastal tree lines and coastal wetlands have the potential to reduce the height of storm surges caused by tropical cyclones that are of moderate severity or less (e.g., not more than Hurricane Category 3) [22, 23], and that they can reduce flooding areas relative to areas that lack a coastal tree line or wetland [25]. Moreover, these studies find that flooding areas are reduced when the width of tree lines [22] or the density of trees increase [26].

The reports mentioned above are mostly case studies of one of the tropical cyclones in the past that approached a coast, caused storm surges to inundate coastal areas, caused damage, and resulted in coastal flooding. However, it is not clear the extent to which the results of any one of such case studies is applicable to other cases. This study therefore aims to explore the potential for coastal tree lines to reduce coastal flooding areas caused by high waves applied to idealized beaches. A numerical model is used for the sensitivity analysis of the geographical factors that affect coastal flooding, which are slope of the beach, bottom friction coefficient, length of the coastal tree line, width of the coastal tree line, and shape of the coastal tree areas. The study results will provide important guidelines for preparing for and alleviating the damage caused by coastal flooding.

## 2. Study Method

This study focuses on coastal flooding, in which the water movement in horizontal direction is more significant than it in vertical direction. Moreover, in order to avoid time consuming in case of large-area computations, a two-dimensional hydrodynamic model was adopted for the study. The model was originally developed at Coastal Engineering Laboratory, Yokohama National University. Boundary conditions and parameter input of the model is modified for this study to simulate flooding situations under various kinds of incident waves and geographic conditions. In the study model, the mass conservation equation and the two-dimensional horizontal momentum equations of water mass, as expressed in Eq. (1) to (3), are solved for the water elevation and momentum fluxes in the  $x$ - and  $y$ -axes.

$$\frac{\partial \eta}{\partial t} + \frac{\partial M}{\partial x} + \frac{\partial N}{\partial y} = 0 \quad (1)$$

$$\frac{\partial M}{\partial t} + \frac{\partial}{\partial x} \left( \frac{M^2}{D} \right) + \frac{\partial}{\partial y} \left( \frac{MN}{D} \right) + gD \frac{\partial \eta}{\partial x} + \frac{gn^2}{D^{7/3}} M \sqrt{M^2 + N^2} = 0 \quad (2)$$

$$\frac{\partial N}{\partial t} + \frac{\partial}{\partial x} \left( \frac{MN}{D} \right) + \frac{\partial}{\partial y} \left( \frac{N^2}{D} \right) + gD \frac{\partial \eta}{\partial y} + \frac{gn^2}{D^{7/3}} N \sqrt{M^2 + N^2} = 0 \quad (3)$$

where  $\eta$  is water surface profile above still water level;  $D$  equals to  $\eta + h$ , where  $h$  is the still water level;  $g$  is acceleration of gravity;  $x$  and  $y$  are horizontal coordinates;  $t$  is time,  $M$  and  $N$  are the  $x$  and  $y$  components of momentum flux, and  $n$  is Manning's friction factor.

In the simulations of flooding situations, conditions and parameters of the models are specified for various case studies. Coastal areas in the study are arbitrarily simulated areas, such that researchers can specify the widths, heights, and slopes of coastal areas. In this study, the areas are specified to have a width along the  $x$ -axis equal to 1,000 m, length along the  $y$ -axis equal to 1,800 m, and default water levels 300 m from the bottom boundaries, which can be divided into dry beaches of 1,500 m and wet beaches of 300 m, as shown in Fig. 1.

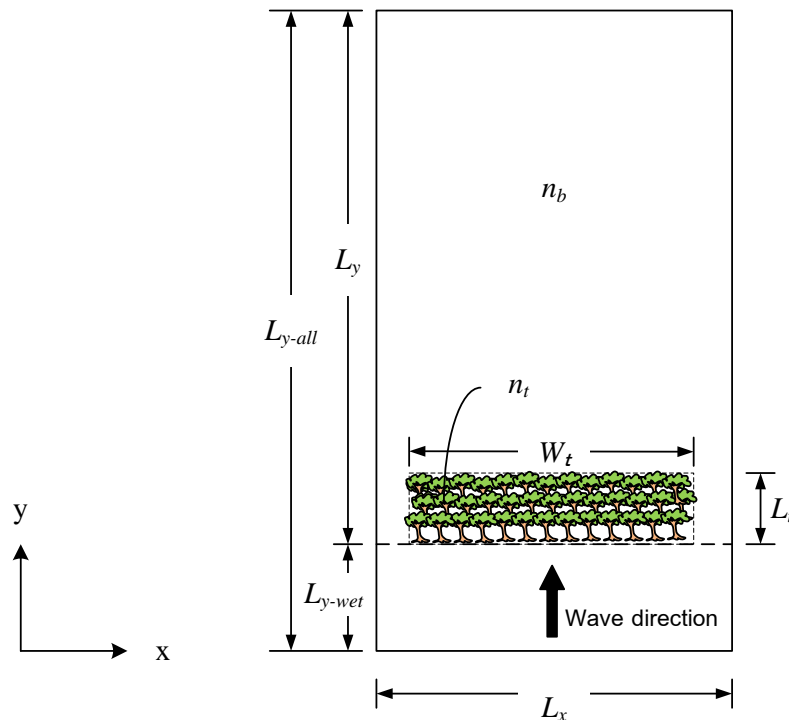


Fig. 1. Sketch of idealized beach used in the study.

The incident waves are specified to have heights ranging from 1 to 5 m. In this study, coastal flooding is simulated for 5 case studies. These are Case Study 1: Study of the Relationship between Flooding Areas and Beach Slopes, Case Study 2: Study of the Relationship between Flooding Areas and Bottom Friction Coefficients, Case Study 3: Study of the Relationship between Flooding Areas and Lengths of Coastal Tree Areas (transverse to the coasts), Case Study 4: Study of the Relationship between Flooding Areas and Widths of Coastal Tree Areas (longitudinal to the coasts), and Case Study 5: Study of the Relationship between Flooding Areas and Shapes of Coastal Tree Areas. The values of the common parameters used in the models are as shown in Table 1. The variable parameters in each case study are as shown in Table 2 to 6.

Table 1. Common parameters used in the study.

Parameters	Symbols	Value	Unit
Width of the beach	$L_x$	1,000	m
Total length of the beach	$L_{y-all}$	1,800	m
Length of the dry beach	$L_y$	1,500	m
Length of the wet beach	$L_{y-wet}$	300	m
Length of the tree area	$L_t$	(varied)	m
Width of the tree area	$W_t$	(varied)	m
x-axis grid size	$\Delta y$	50	m
Time step	$\Delta t$	0.1	sec
Beach slope (default)	$BS$	1:300	
Bottom friction coefficient			
for the beach	$n_b$	0.04	
for the coastal trees	$n_t$	0.20	

Table 2. Variable parameters for the Case Study 1.

Case Study 1: Study of the Relationship between Flooding Areas and Beach Slopes	
Beach slope	$BS = 1:50, 1:75, 1:100, 1:125, 1:150, 1:300$
Wave height (m)	$H = 1, 2, 3, 4, 5$
Study code	C1_BS1- $\otimes\otimes\otimes$ _H $\oplus$ , where $\otimes$ is the beach slope (3 digits) and $\oplus$ is the wave height, for example, C1_BS1-050_H1 or C1_BS1-300_H5.

Table 3. Variable parameters for the Case Study 2.

Case Study 2: Study of the Relationship between Flooding Areas and Bottom Friction Coefficients	
Bottom Friction Coefficient	$n_b = 0.04, 0.10, 0.20$
Wave height (m)	$H = 1, 2, 3, 4, 5$
Study code	C2_NB $\otimes\otimes\otimes$ _H $\oplus$ , where $\otimes$ is the bottom friction coefficient (3 digits) and $\oplus$ is the wave height, for example, C1_NB004_H1 or C1_NB010_H5.

Table 4. Variable parameters for the Case Study 3.

Case Study 3: Study of the Relationship between Flooding Areas and Lengths of Coastal Tree Areas	
Lengths of Coastal Tree Areas (m)	$L_t = 150, 250, 350, 450, 550, 650$ for the wave height of 1 m. $L_t = 200, 400, 600, 800, 950$ for the wave height of 1.5 m. $L_t = 250, 500, 750, 1000, 1250$ for the wave height of 2 m. $L_t = 300, 600, 900, 1200, 1500$ for the wave height of 2.5 m. $L_t = 300, 450, 600, 750, 900, 1050, 1200, 1350, 1500$ for the wave height of 3 m.
Wave height (m)	$H = 1, 1.5, 2, 2.5, 3$
Study code	C3_H $\oplus$ LT $\otimes\otimes\otimes\otimes$ = $\emptyset\emptyset\emptyset$ , where $\oplus$ is the wave height (1 or 2 digits), $\otimes$ is the length of tree area (4 digits) and $\emptyset$ is the percentage of the tree length to the maximum flooding length in the case of no tree (see more details in next section), for example, C3_H1-LT0150=023 or C3_H1.5_LT1500=100.

Table 5. Variable parameters for the Case Study 4.

Case Study 4: Study of the Relationship between Flooding Areas and Widths of Coastal Tree Areas	
Widths of Coastal Tree Areas (m)	$W_t = 200, 400, 600, 800, 1000$
Wave height (m)	$H = 1$
Study code	C4_WT $\otimes\otimes\otimes\otimes$ , where $\otimes$ is the width of tree area.

Table 6. Variable parameters for the Case Study 5.

Case Study 5: Study of the Relationship between Flooding Areas and Shapes of Coastal Tree Areas	
Shapes of Coastal Tree Areas	Shape 1 (P1): 1 set of tree area of 600 m wide and 250 m long Shape 2 (P2): 2 set of tree area of 300 m wide and 250 m long Shape 3 (P3): 3 set of tree area of 200 m wide and 250 m long
Wave height (m)	$H = 1, 2, 3, 4, 5$
Study code	C5_P $\otimes$ , where $\otimes$ is the shape number.

### 3. Results and Discussion

In considering the sensitivity of flooding areas to geographical variables and the characteristics of coastal trees, the characteristics of flooding areas are as follows (see Fig. 2): (1) the maximum length of the flooded area,  $L_f$ , refers to the distance along the y-axis from the initial shoreline to the maximum point of the flooding area, (2) the maximum run-up,  $R_f$ , refers to the vertical level from the still water level to the maximum level of flooding areas, and (3) the percentage of reduction of flood area,  $RA$  (%) is the percentage of the flooding area reduction as given by:

$$RA(\%) = \frac{A_{f-tree} - A_{f-no\ tree}}{A_{f-no\ tree}} \times 100 \quad (4)$$

where  $A_{f-tree}$  is the maximum flooding area with trees and  $A_{f-no\ tree}$  is the maximum flooding area with no tree.

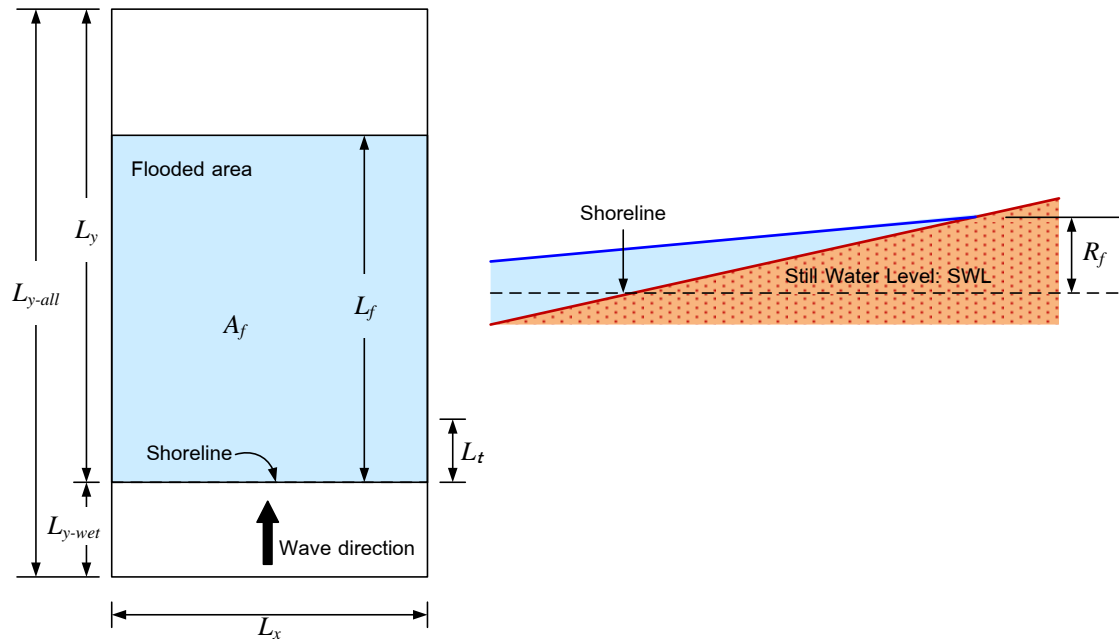


Fig. 2. Sketch of parameters depicting the flooding area.

### 3.1. Case Study of the Relationship between Flooding Areas and Beach Slopes

The results evaluating the relationship between flooding area and slope of the beach for 6 cases, 1:50, 1:75, 1:100, 1:125, 1:150, and 1:300, at maximum wave heights of 1, 2, 3, 4, and 5 m, are shown in Figs. 3 and 4. Figure 3 illustrates the sensitivity of the maximum lengths of flooding areas  $L_f$  to beach slope and wave height. From the graph, it is evident that when wave height increases,  $L_f$  increases non-linearly. The magnitudes of the increase tend to decline as wave heights increase. At the same wave heights,  $L_f$  increase as beach slopes decrease. These characteristics occur because wave energy is transformed into potential energy. For the case of steeper beaches, steeper slopes impede water mass movement, as part of the energy is transformed into potential energy.

Figure 4 illustrates the sensitivity of the maximum flooding run-ups  $R_f$  to wave heights and beach slopes, which is similar to  $L_f$ . As wave heights increase, the maximum run-ups increase because the total energy of the waves increases in a non-linear proportion. The increase tends to be lower when wave heights are larger, in contrast to the effect on the maximum length of flooding area.  $R_f$  decrease as slopes decline because beaches with milder slopes dissipate the wave energy better. Hence, with regard to potential energy in each case, gradual beach slopes disperse more energy, such that less energy will be transformed into potential energy, resulting in lower maximum run-ups.

From the results of simulations above, it can be summarized that beaches with milder slopes will cause larger flooding areas than the beaches with steep slopes. However, with the same water mass of incident waves, shores of beaches with steep slopes will have a higher inundation, which can pose a greater danger to lives.

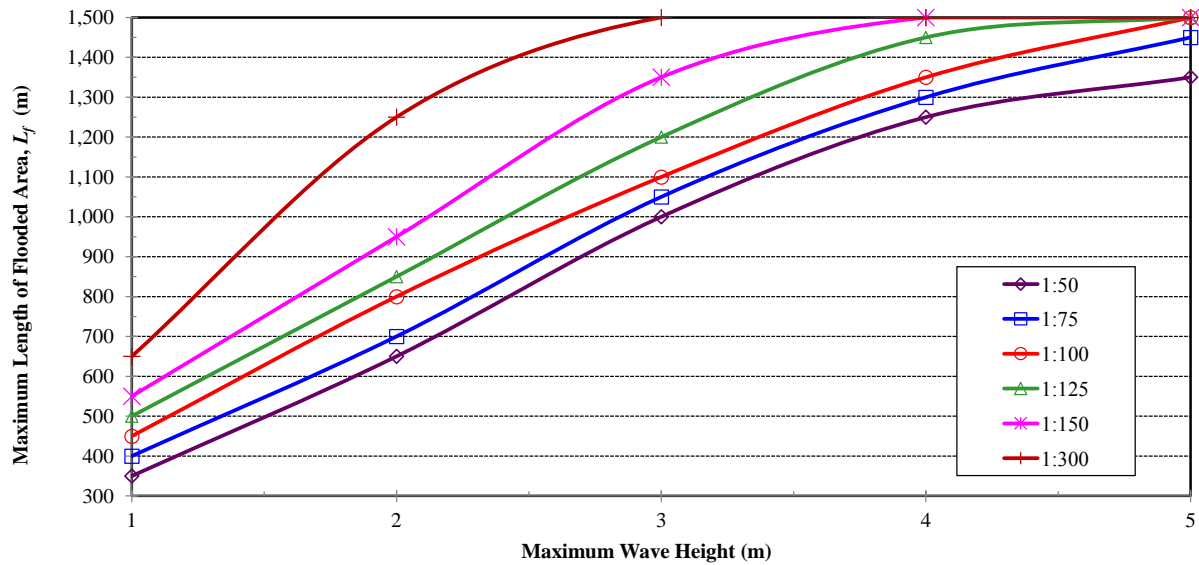


Fig. 3. Relationship between of the maximum lengths of flooding areas  $L_f$ , beach slope and wave heights.

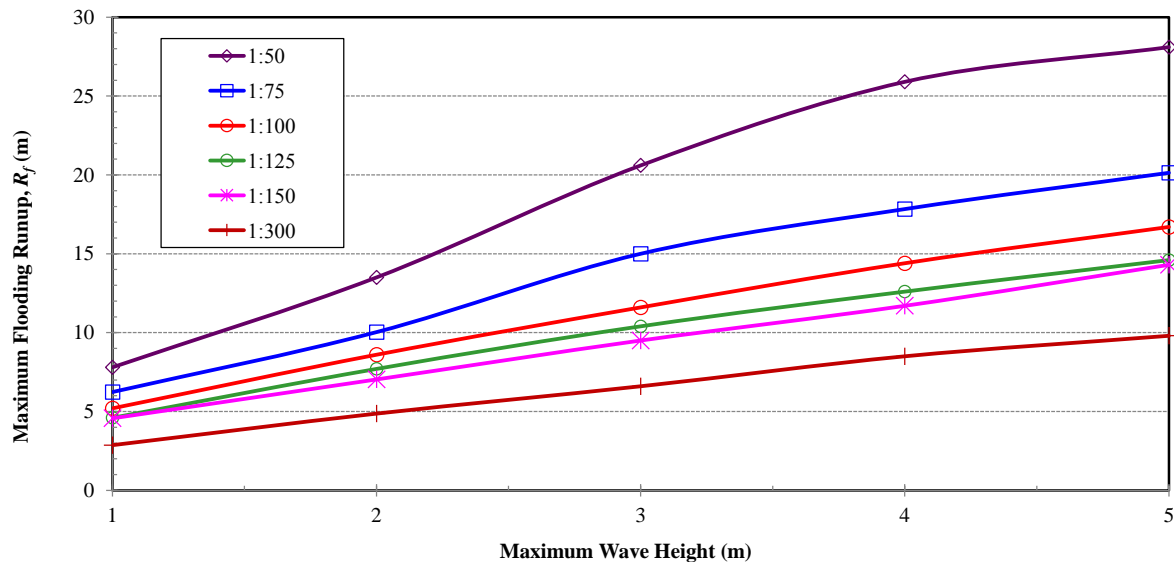


Fig. 4. Relationship between maximum flood run-ups  $R_f$ , beach slope and wave height.

### 3.2. Case Study of the Relationship between Flooding Areas and Bottom Friction Coefficients

The results from the study of the relationship between flooding areas and bottom friction coefficients, which were varied in 3 cases as 0.40, 0.10, and 0.20, are as follows. At maximum wave heights of 1, 2, 3, 4, and 5 m, the relationship is as shown in Figs. 5 and 6. Figure 5 illustrates the relationship between  $L_f$ , bottom friction coefficients and wave heights. The graph shows that when the friction coefficient increases,  $L_f$  will decrease because the increasing friction coefficients cause more friction or drag on the bed, decreasing the momentum of the incident waves. This simulation yields similar results as in the case of beaches with very steep slopes.

Figure 6 illustrates the effects of bottom friction coefficients and wave heights on  $R_f$ . These results have similar characteristics to the cases of Fig. 5: beaches with higher bottom friction coefficients will experience less  $R_f$  because the momentum of wave mass is diminished by the increasing friction.

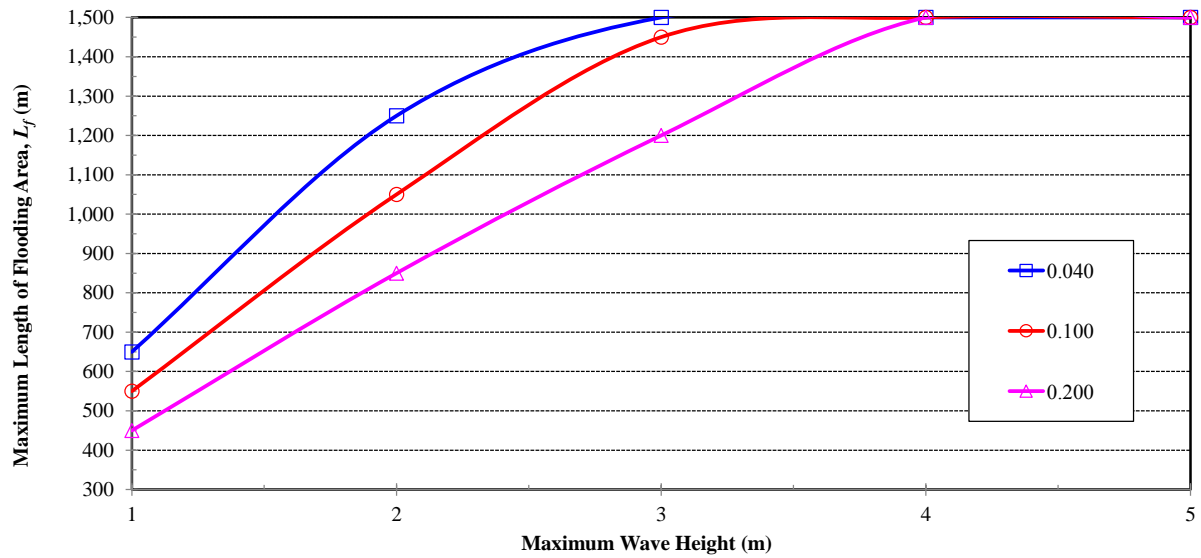


Fig. 5. Relationship between of the maximum lengths of flooding areas  $L_f$ , Manning friction efficient and wave height.

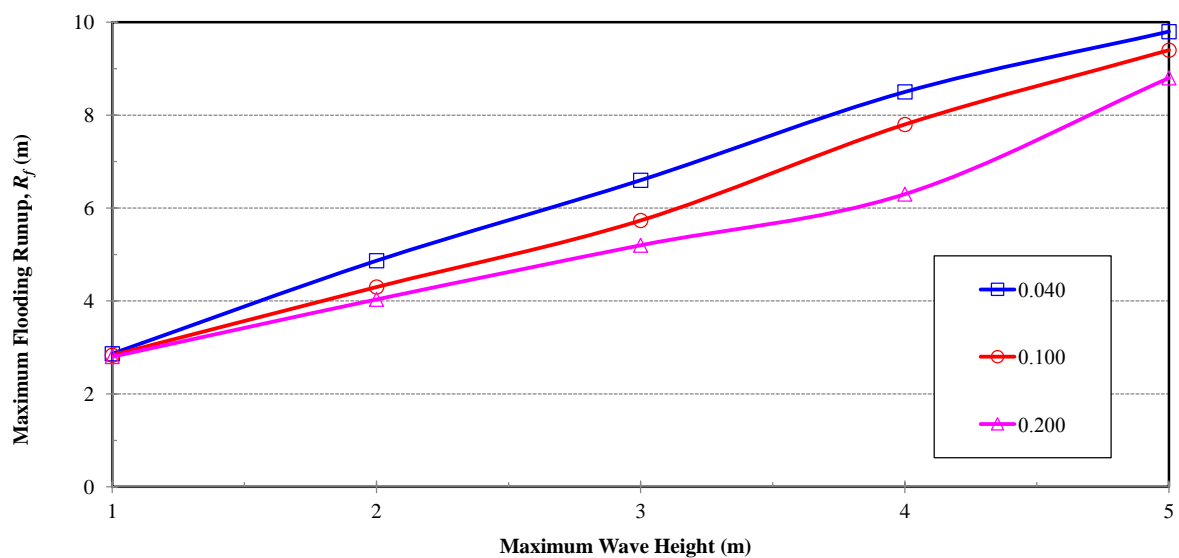


Fig. 6. Relationship between of the maximum lengths of flooding areas  $R_f$ , Manning friction efficient and wave height.

### 3.3. Case Study of the Relationship between Flooding Areas and Lengths of Coastal Tree Areas

The results from the study of the relationship between flooding areas and lengths of coastal tree areas  $L_t$  demonstrate that coastal tree areas can vary the proportions of the flooding areas relative to the maximum flooding area when there are no trees, as shown in Table 7.



Table 7. Variation of the length of coastal tree areas used in the model.

Wave height (m)	Length of maximum flood area without trees $L_f$ (m)	Length of coastal tree areas $L_t$ (m) and percentage of $L_t$ to $L_f$ (%)
1.0	650	150 (23%), 250 (38%), 350 (54%), 450 (69%), 550 (85%), 650 (100%)
1.5	950	200 (21%), 400 (42%), 600 (63%), 800 (84%), 950 (100%)
2.0	1250	250 (20%), 500 (40%), 750 (60%), 1000 (80%), 1250 (100%)
2.5	1500	300 (20%), 600 (40%), 900 (60%), 1200 (80%), 1500 (100%)
3.0	1500	300 (20%), 450 (30%), 600 (40%), 750 (50%), 900 (60%), 1050 (70%), 1200 (80%), 1350 (90%), 1500 (100%)

Figure 7 illustrates the relationship between the percentage of the lengths of coastal tree lines relative to the length of the maximum flooding area without trees and the percentage reduction of flooding area, at wave heights of 1.0, 1.5, 2.0, 2.5, and 3.0 m. The simulated data demonstrate that coastal tree lines can reduce flooding areas; as tree lines lengthen, flooding areas decrease. Tree lines can reduce flooding areas by as much as 31% – 33%. However, in the case of a 3.0-m wave height, a tree line can yield a reduction of flooding area of only 20 %.

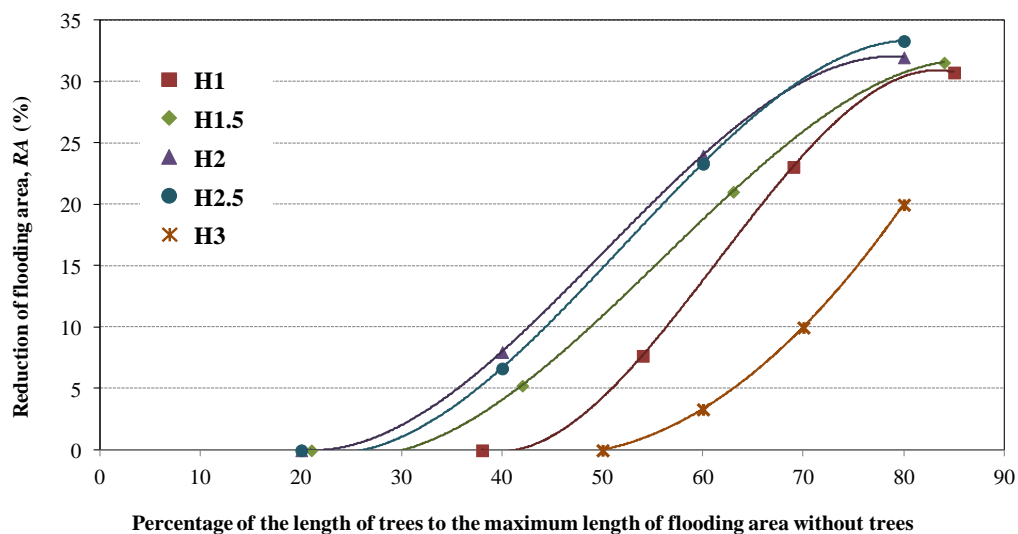


Fig. 7. Reduction of flooding area  $RA(\%)$  and the percentage of the length of trees relative to the maximum length of flooding area without trees.

The percentage reduction in flooding area due to lengths of tree areas relative to the maximum length of flooding area with no trees could be sorted into a descending order for wave heights of 2.0 m, 2.5 m, 1.5 m, 1.0 m, and 3.0 m, in that order, at a percentage length of trees of 50% relative to the length of maximum flooding area without trees. For very high waves, e.g., 3 m, the reduction of flooding areas was lower, as discussed previously. However, the maximum reduction in flooding area does not occur at the lowest wave heights. This is because at lower wave heights, e.g., 1 m, less flooding occurs; therefore, the same percentage of lengths of tree areas to the length of maximum flooding area yields shorter lengths of tree line than in the other cases. Thus, the potential for the tree line to reduce flooding areas cannot be high. This study revealed that potential for tree lines to reduce flooding areas was maximized at a 2-m wave height.

The trend lines in Fig. 7 were generated by the following polynomial equation:

$$y = ax^3 + bx^2 + cx + d \quad (5)$$

where  $x$  is the percentage of the length of trees to the maximum length of flooding area without trees,  $y$  is the reduction of flooding area  $RA(\%)$ ,  $a$ ,  $b$ ,  $c$  and  $d$  are empirical parameters determined by the least squares method and summarized in Table 8.

Table 8. Empirical parameters for Eq. (5).

Wave height (m)	$a$	$b$	$c$	$d$
1.0	-7.48E-04	1.38E-01	-7.42E+00	1.24E+02
1.5	-2.84E-04	4.77E-02	-1.88E+00	2.11E+01
2.0	-3.33E-04	5.00E-02	-1.67E+00	1.60E+01
2.5	-3.47E-04	5.42E-02	-1.94E+00	2.00E+01
3.0	0.00	1.67E-02	-1.50E+00	3.33E+01

Equation (5) with the parameters in Table 8 can be applied to find the most effective length of coastal tree area to reduce flooding area. For example, to reduce the flooding area of 20%, the most effective lengths of coastal tree areas are 427 m, 586 m, 688 m, 833 m and 1198 m (or 65.6%, 61.7%, 55.0%, 55.5% and 79.8% of the maximum length of flooding area without trees) for the cases of different attacking-wave heights of 1, 1.5, 2, 2.5 and 3 m.

Figure 8 illustrates simulated flooding times of 240, 480, 720, 960, and 1200 seconds for the cases C3\_H2\_LT10=040, C3\_H2\_LT15=060 and C3\_H2\_LT20=080 in order to display differences in flooding conditions. In the case of a 2-m wave height and beaches with percentages of length of coastal tree lines to length of maximum flooding area of 40%, 60%, and 80%, Fig. 8 clearly illustrates that longer tree lines have a greater potential to decrease flooding areas, as discussed above. In cases of longer tree lines, tree lines obstruct the movement of water mass to the beaches and cause water levels in vicinity of the front tree lines to increase.

### 3.4. Case Study of the Relationship between Flooding Areas and Widths of Coastal Tree Areas

Results from the study of the relationship between flooding areas and widths of coastal tree areas are illustrated in Fig. 9. The coastal tree areas vary, in the proportion of the width of the study area (1,000 m) from the ratios of widths of tree areas to the study area at 20%, 40%, 60%, 80%, and 100%. The reduction percentage of flooding areas is equivalent to ratios of the flooding areas to the maximum flooding area with no tree.

The calculations demonstrate that, as the widths of coastal tree lines increase, providing more shelter, flooding areas decrease. This relationship is almost, though not exactly, linear. If the relationship is expressed using the polynomial equation as in Eq. (5), each variable can be illustrated as in Fig. 9. The equation can be employed either straightforwardly to evaluate the potential of existing coastal trees to reduce flooding areas or reversely to design the most effective width of coastal tree area to reduce flooding. For example, to reduce the flooding area of 20% for the case of 1 m-attacking-wave height, the most effective width of coastal tree area is 619 m (or 61.9% of the study area of 1000 m).

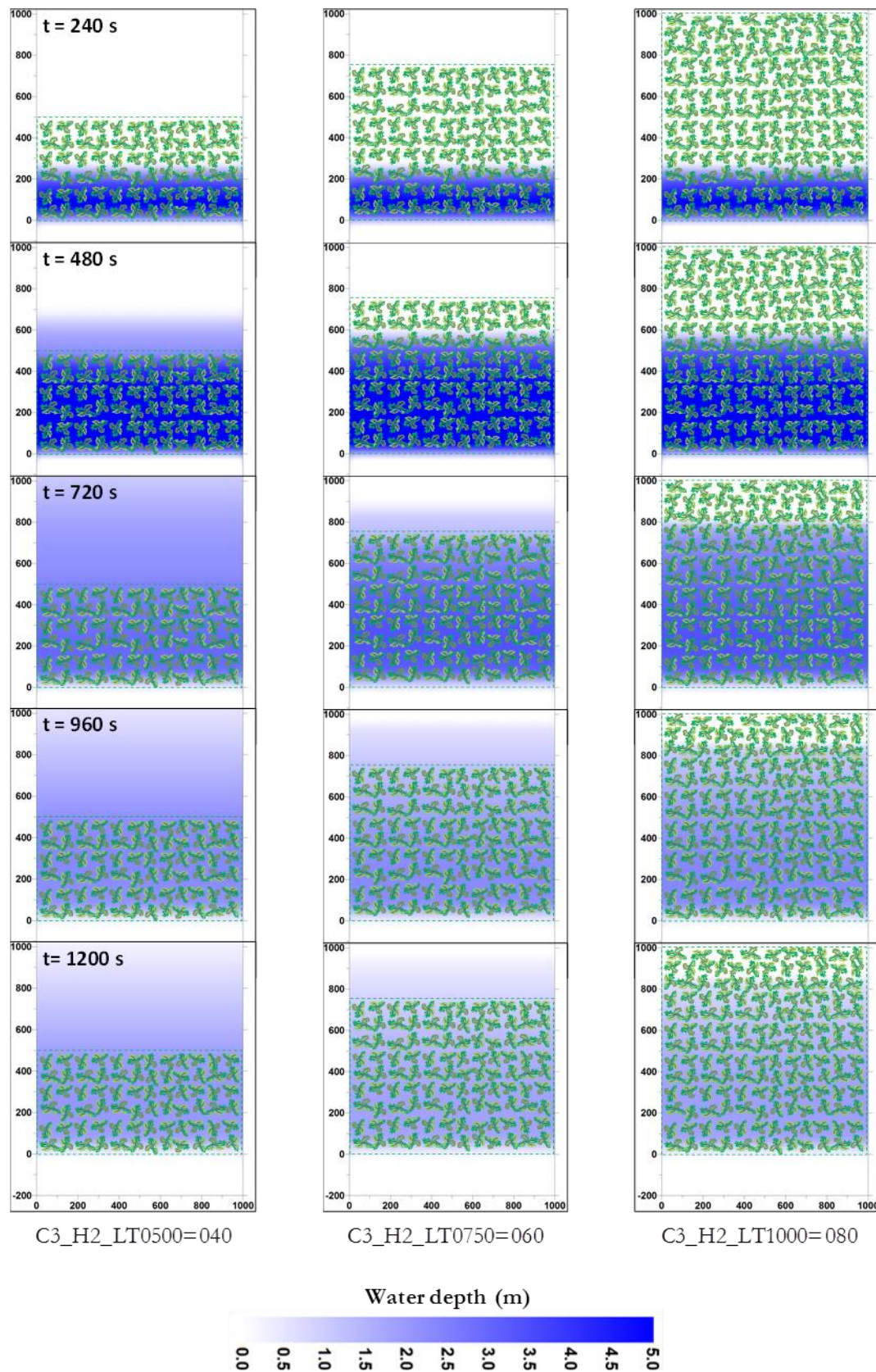


Fig. 8 Simulated flooding areas for the cases C3\_H2\_LT0500=040, C3\_H2\_LT0750=060 and C3\_H2\_LT1000=080 at times of 240, 480, 720, 960, and 1200 seconds.

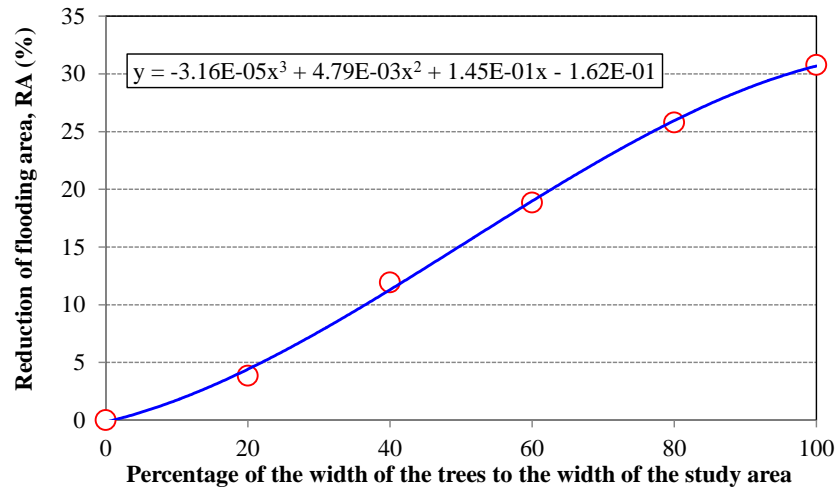


Fig. 9. Relationship between the reduction of flooding areas  $RA(\%)$  and the percentage of the width of tree areas to the width of the study area.

### 3.5. Case Study of the Relationship between Flooding Areas and Shapes of Coastal Tree Areas

The results of three models studying the relationship between flooding areas and shapes of coastal tree areas are shown in Figure 10. The models were as follows: Model No. 1 (P1) – 1 set of tree area of 600 m wide and 250 m long; Model No. 2 (P2) – 2 sets of tree areas of 300 m wide and 250 m long; and, Model No. 3 (P3) – 3 sets of tree areas of 200 m wide and 250 m long. The three shapes have the same total tree areas of 150,000 sq. m. The simulated results revealed that each shape yields a similar reduction of the flooding areas relative to the case of an area with no trees. With Model No. 1, the flooding area was decreased by 19%, while with Model No. 2 and 3 flooding areas were decreased by 15% and 14%, respectively, as shown in Fig. 10.

Figure 11 illustrates simulated flooding times of 120, 240, 360, 480, 600, and 720 seconds for the cases of C5\_P1, C5\_P2 and C5\_P3 to display differences in flood conditions. In the case of 1-m wave height and beaches with coastal tree line areas of Model No. 1, Model No. 2, and Model No. 3, the simulated results clearly show that coastal tree lines can obstruct the wave incident onto the shores well. Areas behind tree lines encounter less flooding. Resistance due to the density of the trees reduces energy and inhibits flood movement, although these effects accumulated flood waters in front of tree lines.

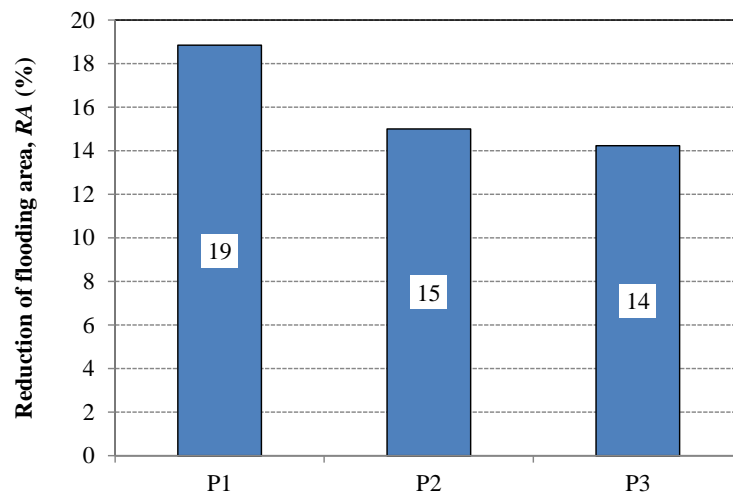


Fig. 10. Relationship between the reduction of flooding areas  $RA(\%)$  and the shapes of coastal tree areas.



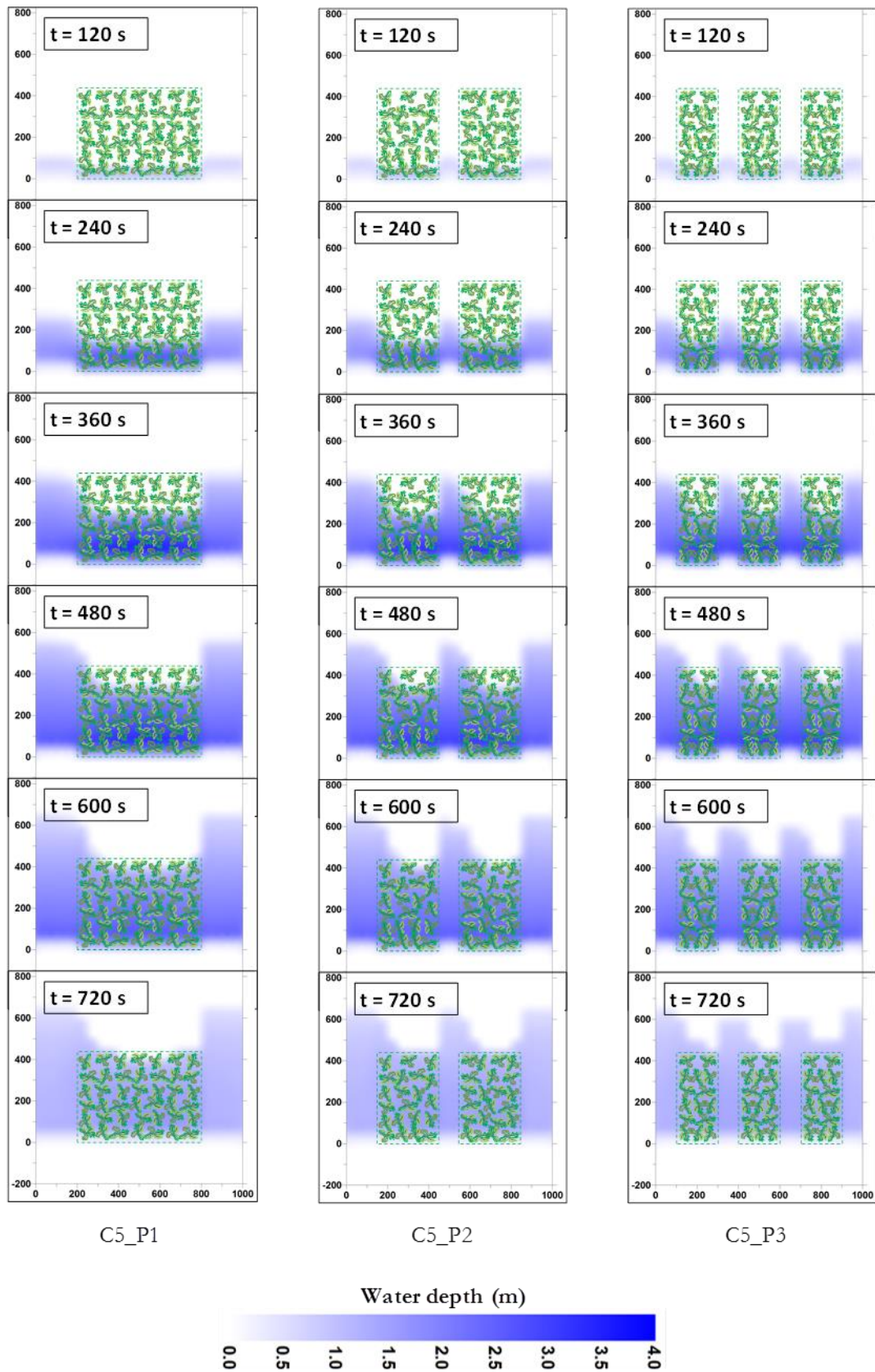


Fig. 11. Simulated flooding areas for the cases of C5\_P1, C5\_P2 and C5\_P3 at time of 120, 240, 360, 480, 600, and 720 seconds.

### 3.6. Recommendation for Future Studies

In this part the further researches regarding the potential of coastal trees to reduce the flooding area due to high waves are proposed as follows:

- (1) Model sensitivity to the interaction among all geological and botanic factors should be analyzed. Furthermore, other interesting factors, for example, the ratio of width-to-length of tree area, non-uniform beach slope, should be taken into account in the future studies.
- (2) Recommended values of bottom friction coefficient representing different bed conditions and various types of coastal trees should be investigated, particularly in the field.
- (3) Guideline of the application of coastal tree areas as natural structures to protect coastal zones or to reduce coastal disasters should be established and implemented.

## 4. Conclusion

Coastal flooding due to very high waves, such as storm surges incident upon coastal areas, was analyzed using a two-dimensional hydrodynamic model. This study evaluated the sensitivity of flooding areas to several geographical factors, including slope of the beach, bottom friction coefficients, length of coastal tree line, width of coastal tree line, and shape of the coastal tree areas. The study results revealed that slopes of beaches significantly affect the magnitude of flooding areas. Beaches with steeper slopes yield smaller flooding areas, while beaches with gradual slopes yield larger flooding areas. This is because with steep slopes, the wave energy incident onto the shores is transformed into potential energy or run-ups. However, with regard to lost energy, the study found that wave energy is more dispersed in beaches with gradual slopes because longer gradient distances along the slopes cause more friction and attenuate more energy. Therefore, beaches with gradual slopes yield lower run-ups.

With regard to bottom friction coefficients, flooding areas decreased as the bottom friction coefficients increased. However, run-ups were found to be deeper in cases of higher bottom friction coefficients because, while the bottom friction resists the movement of flood, the wave water mass is still incident upon the shore, causing more accumulated water and deeper run-ups.

The effects of lengths and widths of coastal tree areas on flooding areas were similar: when the lengths or widths of tree areas increase, the potential to decrease flooding areas increase. In both cases, when tree coverage was high, the maximum flooding area relative to the case of an area with no trees was reduced by 30%. When wave heights were also taken into consideration, coastal tree lines still had some potential to reduce the flooding areas.

For shapes of coastal tree areas at the same controlled total tree areas, it is found that they did not have much of an effect on coastal flooding areas. The continuous tree area models could reduce flooding areas better than the models with small gaps in between the trees.

This study helps elucidate the characteristics of flood movements based on simulated coasts and the potentials of coastal tree lines to reduce coastal flooding areas, providing a basic understanding of these factors for the further study of coastal disaster management.

## Acknowledgement

This work was financially supported by the Research Grant of Burapha University through Higher Education Research Promotion (HERP), Office of the Higher Education Commission (Proposal no. 2554A10862005, Project no. 38048).

## References

- [1] J. C. Doornkamp, "Coastal flooding, global warming and environmental management," *Journal of Environmental Management*, vol. 52, no. 4, pp. 327–333, Apr., 1998.
- [2] IPCC, *Climate Change 2013: The Physical Science Basis. Contribution of Working Group I to the Fifth Assessment Report of the Intergovernmental Panel on Climate Change*. T. F. Stocker, D. Qin, G.-K. Plattner, M. Tignor, S. K. Allen, J. Boschung, A. Nauels, Y. Xia, V. Bex, and P.M. Midgley, Eds. Cambridge, United Kingdom and New York, NY, USA: Cambridge University Press, 2013.

- [3] S. Wang, R. McGrath, J. Hanafin, P. Lynch, T. Semmler, and P. Nolan, "The impact of climate change on storm surges over Irish waters," *Ocean Modelling*, vol. 25, no. 1–2, pp. 83–94, Jul., 2008.
- [4] T. Konishi and Y. Tsuji, "Analyses of storm surges in the western part of the Seto Inland Sea of Japan caused by Typhoon 9119," *Continental Shelf Research*, vol. 15, no. 14, pp. 1795–1823, Dec., 1995.
- [5] M. Y. Zhang and Y. S. Li, "The synchronous coupling of a third-generation wave model and a two-dimensional storm surge model," *Ocean Engineering*, vol. 23, no. 6, pp. 533–543, Aug., 1996.
- [6] F. Shi, W. Sun, and G. Wei, "A WDM method on a generalized curvilinear grid for calculation of storm surge flooding," *Applied Ocean Research*, vol. 19, no. 4, pp. 275–282, Oct.–Dec., 1997.
- [7] J. E. Jones and A. M. Davies, "Storm surge computations for the Irish Sea using a three-dimensional numerical model including wave-current interaction," *Continental Shelf Research*, vol. 18, no. 2–4, pp. 201–251, May, 1998.
- [8] M. Peng, L. Xie, and L. J. Pietrafesa, "A numerical study of storm surge and inundation in the Croatan-Albemarle-Pamlico Estuary System," *Estuarine, Coastal and Shelf Science*, vol. 59, no. 1, pp. 121–137, Jan., 2004.
- [9] P. Lionello, A. Sanna, E. Elvini, and R. Mufato, "A data assimilation procedure for operational prediction of storm surge in the northern Adriatic Sea," *Continental Shelf Research*, vol. 26, no. 4, pp. 539–553, Mar., 2006.
- [10] J. Shen, H. Wang, M. Sisson, and W. Gong, "Storm tide simulation in the Chesapeake Bay using an unstructured grid model," *Estuarine, Coastal and Shelf Science*, vol. 68, no. 1–2, pp. 1–16, Jun., 2006.
- [11] L. Xie, H. Liu, and M. Peng, "The effect of wave–current interactions on the storm surge and inundation in Charleston Harbor during Hurricane Hugo 1989," *Ocean Modelling*, vol. 20, no. 4, pp. 252–269, 2008.
- [12] B. H. Choi, H. M. Eum, and S. B. Woo, "A synchronously coupled tide–wave–surge model of the Yellow Sea," *Coastal Engineering*, vol. 47, no. 4, pp. 381–398, Feb., 2003.
- [13] S. Y. Kim, T. Yasuda, and H. Mase, "Numerical analysis of effects of tidal variations on storm surges and waves," *Applied Ocean Research*, vol. 30, no. 4, pp. 311–322, Oct., 2008.
- [14] H. Madsen and F. Jakobsen, "Cyclone induced storm surge and flood forecasting in the northern Bay of Bengal," *Coastal Engineering*, vol. 51, no. 4, pp. 277–296, Jun., 2004.
- [15] W. P. Huang, C. A. Hsu, and J. Z. Yim, "Numerical studies on typhoon surges in the Northern Taiwan," *Coastal Engineering*, vol. 54, no. 12, pp. 883–894, Dec., 2007.
- [16] M. F. Karim and N. Mimura, "Impacts of climate change and sea-level rise on cyclonic storm surge floods in Bangladesh," *Global Environmental Change*, vol. 18, no. 3, pp. 490–500, Aug., 2008.
- [17] P. Pokharel, M. Takeda, and N. Matsuo, "Inundation analysis of the effectiveness of an estuary gate in Hori River," *Journal of Hydro-environment Research*, vol. 2, no. 4, pp. 228–238, Apr., 2009.
- [18] K. Kathiresan and N. Rajendran, "Coastal mangrove forests mitigated tsunami," *Estuarine, Coastal and Shelf Science*, vol. 65, no. 3, pp. 601–606, Nov., 2005.
- [19] J. E. Vermaat and U. Thampanya, "Mangroves mitigate tsunami damage: A further response," *Estuarine, Coastal and Shelf Science*, vol. 69, no. 1–2, pp. 1–3, Aug., 2006.
- [20] D. M. Alongi, "Mangrove forests: Resilience, protection from tsunamis, and responses to global climate change," *Estuarine, Coastal and Shelf Science*, vol. 76, no. 1, pp. 1–13, Jan., 2008.
- [21] H. Yanagisawa, S. Koshimura, K. Goto, T. Miyagi, F. Imamura, A. Ruangrassamee, and C. Tanavud, "The reduction effects of mangrove forest on a tsunami based on field surveys at Pakarang Cape, Thailand and numerical analysis," *Estuarine, Coastal and Shelf Science*, vol. 81, no. 1, pp. 27–37, Jan., 2009.
- [22] N. M. Loder, J. L. Irish, M. A. Cialone, and T. V. Wamsley, "Sensitivity of hurricane surge to morphological parameters of coastal wetlands," *Estuarine, Coastal and Shelf Science*, vol. 84, no. 4, pp. 625–636, Oct., 2009.
- [23] K. Zhang, H. Liu, Y. Li, H. Xu, J. Shen, J. Rhome, III., and T. Smith, "The role of mangroves in attenuating storm surges," *Estuarine, Coastal and Shelf Science*, vol. 102–103, pp. 11–23, May 2012.
- [24] H. Liu, K. Zhang, Y. Li, and L. Xie, "Numerical study of the sensitivity of mangroves in reducing storm surge and flooding to hurricane characteristics in southern Florida," *Continental Shelf Research*, vol. 64, pp. 51–65, Aug., 2013.
- [25] T. V. Wamsley, M. A. Cialone, J. M. Smith, J. H. Atkinson, and J. D. Rosati, "The potential of wetlands in reducing storm surge," *Ocean Engineering*, vol. 30, no. 1, pp. 311–322, Jan., 2010.
- [26] S. Temmerman, M. B. De Vries, and T. J. Bouma, "Coastal marsh die-off and reduced attenuation of coastal floods: A model analysis," *Global and Planetary Change*, vol. 92–93, no. 4, pp. 267–274, Jul., 2012.

